Energy Proceedings
Vol 26, 2022
ISSN 2004-2965

Numerical Study of the Thermal-Hydraulic Performance of Water-Based Al_2O_3 - Cu Hybrid Nanofluids in a Double-Layer Microchannel Heat Sink

Omosehin OS [1,2], Adelaja AO[1*], Olakoyejo OT[1], Oluwatusin OO[1], Oyekeye OM[1], Abolarin SM[3**]

1 Department of Mechanical Engineering, University of Lagos, Akoka, Yaba, Lagos State, 101017, Nigeria

2 Department of Aeronautics and Astronautics Engineering, Lagos State University, Epe Campus, Lagos State, Nigeria

3 Department of Engineering Science, University of The Free State, Bloemfontein, 9300, South Africa

*Corresponding Author: aadelaja@unilag.edu.ng

** Alternative Corresponding Author: abolarinsm@ufs.ac.za

ABSTRACT

In this work, a numerical study is conducted to investigate the effects of hybrid nanofluid (Al_2O_3-Cu/water) on the thermal and hydraulic performance of a three-dimensional double-layer counterflow microchannel heat sink. The heat sink comprises a silicon block to which a constant heat flux of q = 1.0 MW/m^2 is applied at the base. Different volume concentrations of alumina and copper nanoparticles are considered, with the Reynolds number varying between 200 and 1000. The conjugate heat transfer problem is solved numerically using the two-phase Eulerian-Eulerian model in ANSYS – Fluent environment. Experimental validation shows a good agreement between the numerical models and the experiment. Nanofluids exhibit higher heat transfer coefficients and pressure drops than the base fluid; however, nanoparticle hybridization has a minimal effect on the pressure drop.

Keywords: Hybrid nanofluids, thermal performance, double-layer microchannel heat sink, hydraulic characteristics

1. INTRODUCTION

Cooling devices for better performance has been a big challenge in electronic industries. Conventional fluids like water, glycol, refrigerants, etc., were once adopted to improve the thermal performance of electronic devices. Today, they have become inadequate to provide the desired heat exchange result due to the emergence of compact electronic technologies. Hence the use of nanofluids as cooling agents is of great advantage because of their increased thermal performances and efficiencies via the relative movement between the base fluid and the suspended nanoparticles Pinto and Fiorelli [1]. The suspended nanoparticles in the base fluid can be mono or hybrid nanofluids. Selvakumar and Suresh [2] applied a hybrid nanofluid (Al_2O_3-Cu/water) to an electronic heat sink of a thin-channel copper block. The result showed a significant heat transfer coefficient enhancement by the hybrid nanofluid compared with the base fluid. Wei et al. [3] conducted experimental and numerical studies on a stacked microchannel heat sink and reported that more uniformity in temperature distribution was observed with the counterflow arrangement of coolant compared with the parallel flow. Sarvar-Ardeh et al. [4] adopted a composite nanofluid (Al_2O_3-SiO_2/water and Al_2O_3-Cu/water) with temperature-dependent properties in a double-layered microchannel. They reported that Al_2O_3-SiO_2/water had better thermal performance than Al_2O_3-Cu/water. The thermal performance of porous double-layer MCHS was investigated by Ghahremannezhad et al. [5]. An enhanced thermal characteristic sensitive to the solid porous thickness was observed and reported.

The current study is motivated by the limited numerical investigations using the two-phase Eulerian-Eulerian approach in ANSYS – Fluent environment to study the thermal-hydraulic performance of hybrid nanofluid in a double-layer microchannel heat sink. This research will further expand the numerical database in MCHS.

2. GEOMETRY DESCRIPTION

The schematic diagram of a double-layer microchannel heat sink is shown in Fig. 1, and the dimensions are in Table 1. It consists of the fluid and solid domains for numerical computation. The solid domain comprises a silicon block with a uniform heat flux applied

to the base. The hybrid nanofluid flows in the direction of the arrows through the channel.

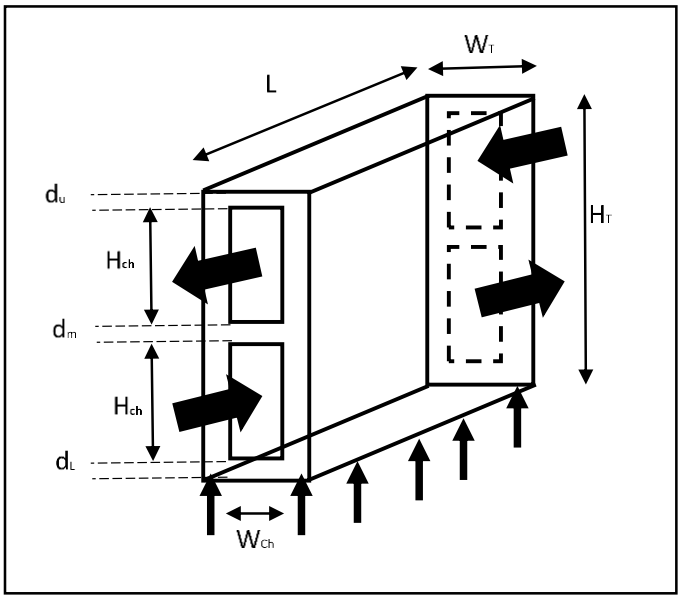

Fig. 1 Schematic diagram of the heat sink

3. GOVERNING EQUATION

This work presents a numerical study of laminar, steady-state, incompressible, and three-dimensional Eulerian-Eulerian two-phase flow in a double-layer microchannel counterflow configuration. The numerical model presents the primary phase (pure water) and two secondary phases (alumina and copper particles). The thermal properties of the primary and secondary phases are presented in Table 2, and the conservation equations are shown below.

3.1 Mass conservations

Primary phase (pure water)

$$\nabla.\left(\rho_1\alpha_1\vec{V}_1\right)=0 \quad (1)$$

Secondary phase (alumina particles)

$$\nabla.\left(\rho_2\alpha_2\vec{V}_2\right)=0 \quad (2)$$

Secondary phase (copper particles)

$$\nabla.\left(\rho_3\alpha_3\vec{V}_3\right)=0 \quad (3)$$

Where ρ , α and $\vec{V}$ are the density, volume concentration, and velocity vector, respectively. 1, 2, and 3 represent the primary phase (water) and secondary particulate phases of alumina and copper, respectively.

$$\alpha_1+\alpha_2+\alpha_3=1 \quad (4)$$

3.2 Momentum conservation equations

The momentum conservation equations of the base fluid and nanoparticles are presented in Eq. (5) to Eq. (7)

Primary phase (pure water)

$$\nabla.\left(\rho_1\alpha_1\vec{V}_1\vec{V}_1\right)=-\alpha_1\nabla\mathrm{P}+\nabla.\left[\alpha_1\mu_1\left(\nabla\vec{V}_1+\nabla\vec{V}_1^{T}\right)\right]+F_d+F_{VM} \quad (5)$$

Secondary phase (alumina particles)

$$\nabla.\left(\rho_2\alpha_2\vec{V}_2\vec{V}_2\right)=-\alpha_2\nabla\mathrm{P}+\nabla.\left[\alpha_2\mu_2\left(\nabla\vec{V}_2+\nabla\vec{V}_2^{T}\right)\right]-F_d-F_{VM}+F_{col} \quad (6)$$

Secondary phase (copper particles)

$$\nabla.\left(\rho_3\alpha_3\vec{V}_3\vec{V}_3\right)=-\alpha_3\nabla\mathrm{P}+\nabla.\left[\alpha_3\mu_3\left(\nabla\vec{V}_3+\nabla\vec{V}_3^{T}\right)\right]-F_d-F_{VM}+F_{col} \quad (7)$$

Where P, μ, F_{VM}, F_d and F_{col} are the pressure, dynamic viscosity, virtual mass, drag, and particle-to-particle interaction forces, respectively.

3.3. The energy conservation equations

The energy conservation equations, neglecting the viscous dissipation and radiation, are thus given in Eqs. (8) to (10).

Primary phase (pure water)

$$\nabla.\left(\rho_1\alpha_1Cp_1T_1\vec{V}_1\right)=\nabla.\left(\alpha_1K_1\nabla T_1\right)-Q_h \quad (8)$$

Secondary phase (alumina particles)

$$\nabla.\left(\rho_2\alpha_2Cp_2T_2\vec{V}_2\right)=\nabla.\left(\alpha_2K_2\nabla T_2\right)+Q_h \quad (9)$$

Secondary phase (copper particles)

$$\nabla.\left(\rho_3\alpha_3Cp_3T_3\vec{V}_3\right)=\nabla.\left(\alpha_3K_3\nabla T_3\right)+Q_h \quad (10)$$

Where *T, K, C_p, Q_h* are the temperature, thermal conductivity specific heat capacity, and volumetric rate of energy transfer between the primary and each secondary phase (alumina and copper particles), and it is expressed as

$$Q_h=h_{p,1}\frac{6\alpha_p}{d_p}\left(T_p-T_1\right) \quad (11)$$

Where *h, d,* and subscript *p* are the heat transfer coefficient, diameter, and particulate, respectively

3.4. The conservative energy equation for the solid wall domain

$$K_s\nabla^2T_s=0 \quad (12)$$

Subscript s represents solid.

3.5. Governing boundary conditions

All the solid domain boundaries are considered adiabatic except for the bottom of the microchannel, which is subject to a constant heat flux of 1.0 MW/m^2.

Inlet conditions

$T_{x=0} = T_{in}$= 25°C Bottom channel (13a)

$T_{x=L} = T_{in}$= 25°C Top channel (13b)

$V_{x=0} = V_{in}$ (uniform axial velocity for both base fluid and particulate phases at bottom channel) (14)

$V_{x=L} = -V_{in}$ (uniform axial velocity for both base fluid and particulate phases at the top channel) (15)

Outlet conditions

An ambient outflow condition was applied at the outlet.

Channel bottom (constant heat flux)

$$-k_s \frac{\partial T_S}{\partial n} = q^{ii} \quad (16)$$

Interface conditions

$$T_s = T_f \quad (17)$$

$$-k_s \frac{\partial T_S}{\partial n} = -k_f \frac{T_f}{\partial n} \quad (18)$$

The following parameters are used to investigate the performance of the double-layer microchannel heat sink.

3.6. Average Nusselt number definition

The average Nusselt number (Nu_{avg}) of the flow field is defined as

$$Nu_{avg} = \frac{q^{ll} D_h}{k_f (T_w - T_{in})} \quad (19)$$

Where k_f is the thermal conductivity of the liquid as adopted by [4] and [5].

T_w is the wall temperature at the center of the heated base. T_{in} is the inlet temperature and D_h hydraulic diameter.

3.7. Pressure drop (Δp) deduction

The difference between the top and bottom channel's upstream and downstream pressure is obtained from numerical simulation. The total pressure drop is the addition of the pressure drop at the top and bottom of the microchannel. The upstream and downstream pressures, p_{in} and p_{out} are the area-weighted average pressures at the inlet and outlet.

$$\Delta p_{top} = p_{in} - p_{out} \quad (20)$$

$$\Delta p_{bottom} = p_{in} - p_{out} \quad (21)$$

$$\Delta p_{total} = \Delta p_{top} + \Delta p_{bottom} \quad (23)$$

4. MODEL VALIDATION

An experimental result (83ml/min) from the literature [3] is used to validate the model developed in ANSYS. The numerical result from the ANSYS model is compared with the experimental result of the double-layer counterflow microchannel heat sink, as shown in Fig 2. The comparison is made for single-phase laminar flow with water as the cooling agent and uniform velocity and temperature assumed at the channel's inlet. Uniform heat flux is applied at the bottom with the symmetric condition at the vertical midpoint of the channel. The numerical result agrees with the experimental result in the literature.

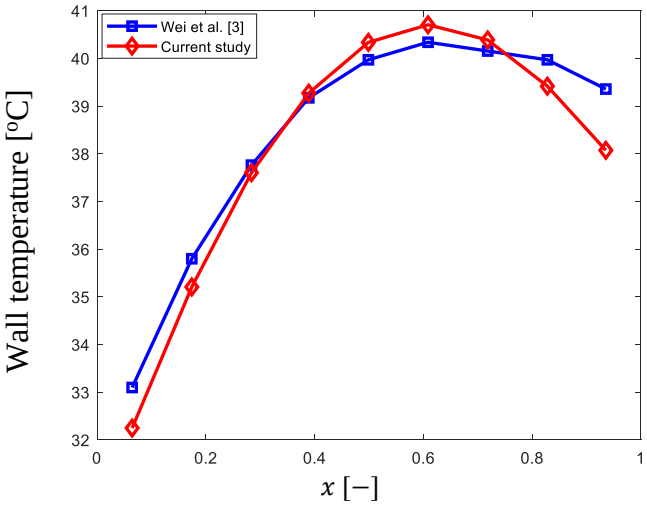

Figure 2 comparison of the present study for wall temperature distribution with the experimental result of Wei et al. [3]

5. GRID INDEPENDENCE TEST

A Grid independence study is conducted using the base fluid (pure water) as the cooling liquid at a Reynolds number of 200. The maximum substrate temperature is monitored to test the grid independence of the different mesh element sizes until there is no significant change in substrate temperature value. A computational grid of element size 1862303 and a percentage change of 0.000064% is sufficient for this study in other to minimize computational time. The percentage change in the substrate temperature between two successive grid

element sizes is computed as $\Delta T = \frac{T_2 - T_1}{T_1}\%$ with convergence criteria of 10^{-6} to control the numerical solution. The summary is shown in Table 3.

Table 1 *Geometry dimensions*

$H_T(\mu m)$	1100	$d_M(\mu m)$	50
$W_T(\mu m)$	150	$d_U(\mu m)$	50
$W_{CH}(\mu m$	100	$H_{CH}(\mu m$	450
$d_L(\mu m)$	100	$L\ (\mu m)$	10000

Table 2 *Thermo-physical properties of pure water, copper and alumina particles*

Materials	$\rho(kg/m^3)$	$C_p(J/kg.K)$	$k(W/m.K)$	$\mu(kg/m.s)$
Pure water	999.1	4184	0.5769	Temperature-dependent
Alumina	3970	765	36	--
Copper particles	8933	385	400	--

Table 3 *Grid independent test*

Element size	Substrate Temperature	$\Delta T(\%)$ in Substrate Temperature
535873	310.5453	-
1092281	310.5798	0.0111
1660105	310.6031	0.0075
1862303	310.6033	0.000064
3822817	310.6035	0.000064

6. RESULT AND DISCUSSION

The effect of hybrid nanofluid on Nusselt Number is presented in Fig 3. Mono and hybrid nanofluids have higher Nusselt numbers than the base fluid. This can be attributed to decreased thermal boundary layer and higher axial conduction at the microchannel's heated base. Also, the Brownian motion of the nanoparticles enhances the thermal conductivity of the heat transfer fluid. However, increasing the concentration of copper particles results in a more significant reduction in the thermal boundary layer due to a further increase in the thermal conductivity; hence, a hybrid nanofluid with a higher concentration of copper nanoparticles produces a higher Nusselt number.

The effect of hybrid nanofluids on pressure drop is presented in Fig 4. Generally, pressure drop increases with an increase in the flow velocity of the heat transfer fluid. However, the presence of nanoparticles in the base fluid (mono and hybrid nanofluid) increases the viscosity and density of the heat transfer fluid. This explains why the mono and hybrid nanofluids produce higher pressure drops along the channel flow path than the base fluid. Also, it is observed that increasing the concentration of copper nanoparticle result in a very small change in pressure drop.

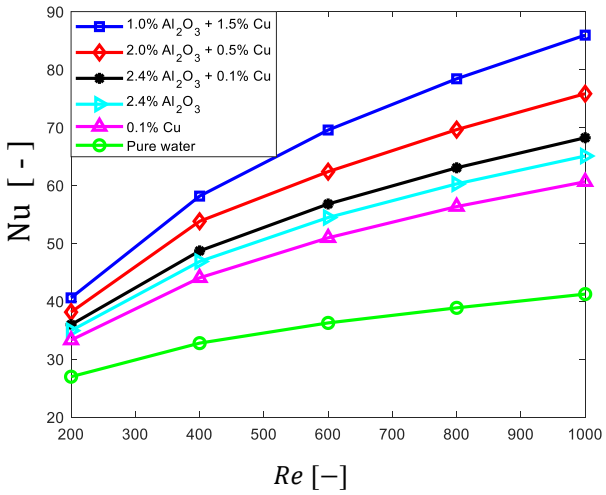

Fig 3. Effect of hybrid nanofluids on Nusselt Number

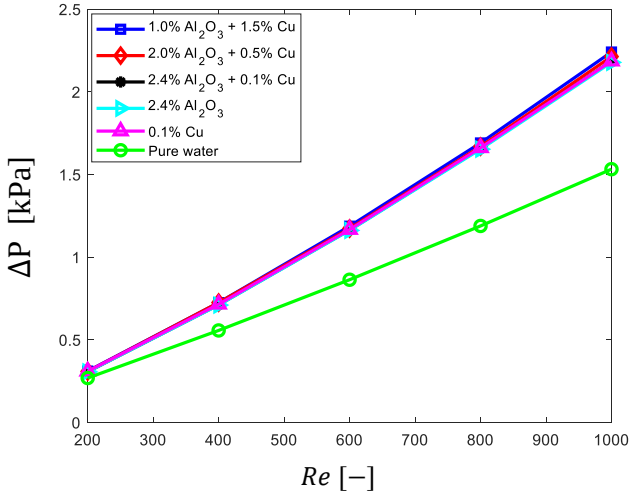

Fig 4. Effect of hybrid nanofluids on pressure drop.

7. CONCLUSION

The thermal and hydraulic performance of water-based Al_2O_3 - Cu hybrid nanofluids in a double-layer microchannel heat sink is numerically investigated using an Eulerian - Eulerian two-phase flow approach in ANSYS

– Fluent environment. It is observed that hybrid nanofluids with the highest concentration of copper particles produce the highest Nusselt number with significant high pressure drops compared with the base fluid. Hybridization of the nanoparticles, irrespective of the concentration of copper nanoparticles, does not significantly affect the pressure drop.

ACKNOWLEDGEMENT

The authors appreciate the support from the University of Lagos, Nigeria, and University of the Free State, South Africa, to present this paper at ICAE2022.

REFERENCE

[1] Pinto RV, Fiorelli FAS. Review of the mechanisms responsible for heat transfer enhancement using nanofluids. Appl Therm Eng 2016;108:720-739.

[2] Selvakumar P, Suresh S. Use of Al 2 O 3-Cu/water hybrid nanofluid in an electronic heat sink. IEEE Trans. Components, Packag. Manuf. Technol 2012; 2(10): 1600-1607

[3] Wei X, Joshi Y, Patterson MK. Experimental and numerical study of a stacked microchannel heat sink for liquid cooling of microelectronic devices. J Heat Transfer 2007; 1432-1444.

[4] Sarvar-Ardeh S, Rafee R, Rashidi S. Hybrid nanofluids with temperature-dependent properties for use in double-layered microchannel heat sink; hydrothermal investigation. J Taiwan Inst. Chem. Eng 2021; 124: 53-62.

[5] Ghahremannezhad A, Xu H, Alhuyi Nazari M, Hossein Ahmadi M, Vafai K. Effect of porous substrates on thermohydraulic performance enhancement of double layer microchannel heat sinks. Int. J. Heat Mass Transf 2019; 131: 52-63.